Systematic Magnetic and Dielectric Investigations of Aluminum Doped Iron Oxide Thin Films

Aseya Akbar[1)], Saira Riaz[2)], S. Sajjad Hussain[3)*], Shahid Atiq[4)], Y.B. Xu[5)] and Shahzad Naseem[6)]

[1), 2), 3), 4), 6)] *Centre of Excellence in Solid State Physics, University of the Punjab, Lahore, Pakistan*
[5)] *Department of Electronics, University of York, UK*
[2)] saira.cssp@pu.edu.pk

ABSTRACT

Iron oxide is material of interest because of its use in spintronic devices. Among various phases of iron oxide Fe_2O_3 is the most stable form, which shows antiferromagnetic or weak ferromagnetic behavior at room temperature. Aluminum (Al) is doped in Fe_2O_3 to enhance dielectric and magnetic properties. Presence of diffraction peaks at (012), (110), (006), (202), (024), (214) and (217) planes indicate the formation of hematite (α-Fe_2O_3). No peaks corresponding to aluminum or aluminum oxide are observed. Shift of peak positions slightly to higher angles is due to smaller ionic radius of Al^{3+} (0.53Å) as compared to Fe^{3+} (0.74Å). Dielectric constant and tangent loss illustrate normal dispersion behavior that agrees well with Maxwell Wagner model. Dielectric constant increases from 49.9 to 51.73 (log *f* = 4.0) as dopant concentration is increased to 6%. Further increase in dopant concentration results in decrease in dielectric constant due to increase in strain. Increase in conductivity of Al doped α-Fe_2O_3 thin films with increase in dopant concentration makes these films appropriate for high density recording media. Ferromagnetic behavior is observed for Al doped α-Fe_2O_3 thin films.

1. INTRODUCTION

In the last decade, transition metal oxides have been given considerable attention owing to their application in magnetic sensors, data storage devices, spintronic devices, photoelectrochemical water splitting and catalytic applications (Ubale and Belkhedkar 2015, Kment et al. 2015, Ahn et al. 2015, Phuan et al. 2015). Among various materials, iron oxide is a capable applicant owing to the fact that its semiconducting and magnetic properties can be tuned by introduction of various dopants (Suresh et al. 2012, Martis et al. 2013).

Iron oxide has 3 important crystallographic phases namely magnetite (Fe_3O_4), maghemite (γ-Fe_2O_3) and hematite (α-Fe_2O_3). α-Fe_2O_3 is low-cost and plentiful in nature with semiconducting properties. It exhibits a band gap of 2.2eV (Huda et al. 2010, Rivera et al. 2012). Its unit cell can be illustrated as hexagonal system. Lattice

parameters are “a=5.03Å” and “c=13.75Å” (Rivera et al. 2012). It can be portrayed as rhombohedral with two formula units. Lattice parameters for such system are “a=5.43Å” and “α=55˚18'” (Rivera et al. 2012). Lattice is comprised of hexagonal closed pack oxygen anions (Rivera et al. 2012). Hematite is antiferromagnetic with Neel temperature of 955K. Below temperature of 260K (Morin Temperature) modification from antiferromagnetic to weak ferromagnetic behavior can be observed. This changeover in magnetic properties is because of canting in spins in hematite crystal structure (Rivera et al. 2012, Shimomura et al. 2015, Levinson 1971).

Trivalent cations are most significant for doping purposes amongst which aluminum (Al^{3+}) is a vital candidate (Bamdad and Ghotbi 2012). Despite the advantages of similar valence state, Al-doped Fe_2O_3 is given very little attention particularly the studies regarding dielectric and magnetic properties are tremendously limited.

We here report preparation and characterization of aluminum doped α-Fe_2O_3 thin films using low cost and application oriented sol-gel method. Dopant concentration was varied as 2%, 6% and 10%. Modifications in various properties are linked with occupation of dopant in α-Fe_2O_3 lattice.

2. EXPERIMENTAL DETAILS

Undoped and aluminum doped α-Fe_2O_3 thin films were synthesized with sol-gel spin coating technique. Iron nitrate ($Fe(NO_3)_3.9H_2O$) and aluminum nitrate ($Al(NO_3)_3.9H_2O$) were used as precursors whereas water and ethylene glycol were used as solvents. $Fe(NO_3)_3.9H_2O$ was dissolved in solvent and heat treated to synthesize iron oxide sol. Further elaboration of sol-gel process has been published elsewhere (Riaz et al. 2014a, Akbar et al. 2014b). For aluminum doping, $Al(NO_3)_3.9H_2O$ was mixed in the solvent. This solution was then mixed in the sol. Dopant concentration was varied as 2%, 6% and 10%. Films were deposited on copper substrate. Before deposition, etching and cleaning of copper substrates was done. Copper substrates were etched using hydrochloric acid and then washed with DI water (Asghar et al. 2006a,b). Films were deposited using Delta 6RC spin coater. These films were characterized with the help of XRD, VSM and impedance analyzer.

3. RESULTS AND DISCUSSION

Fig. 1 shows XRD plots of Al-doped iron oxide thin films. Peaks are labeled for α-Fe_2O_3. No peaks corresponding to Al_2O_3 can be seen thus depicting that Al^{3+} has replaced iron in the lattice. Al^{3+} cations have ionic radius of 67.5pm that is less than that of Fe^{3+} cations (74pm). This leads to diminution of unit cell that is in accordance to Bragg’s law (Cullity 1956). Shifted position of (202) and (024) diffraction peaks to higher angles can be seen in Fig. 1(a-c). Ratio of ionic radii of Al^{3+} and Fe^{3+} cations is 0.912. This value is larger than the limit for formation of solid solution (Cullity 1956). Therefore, Al^{3+} cations take up the substitutional sites instead of interstitial sites. However, at dopant concentration of 10% possibility that dopant atom dwell on the grain boundaries become high (Biju and Wen 2013). This leads to damage of crystalline order with decrease in crystallinity of α-Fe_2O_3 thin films.

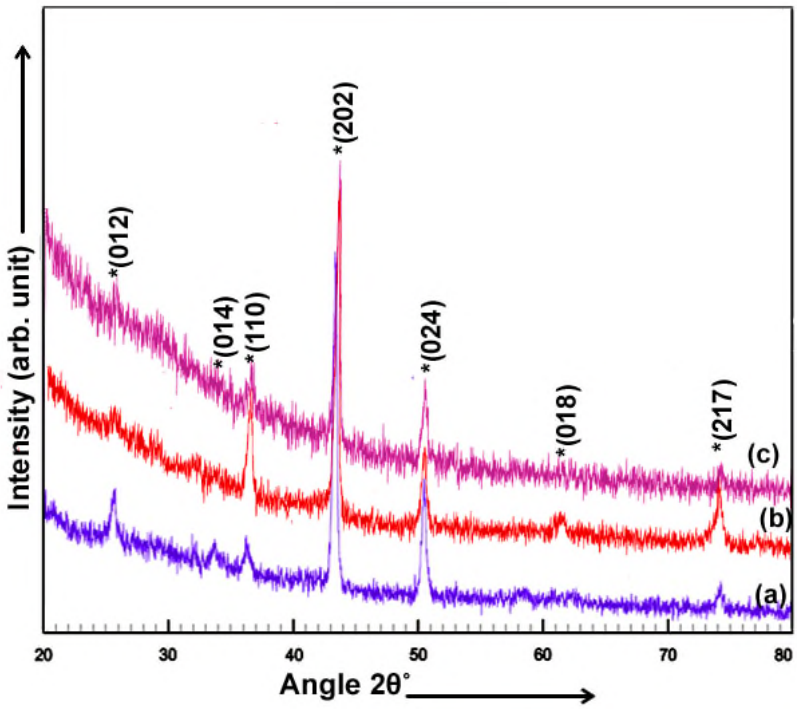

Fig. 1 XRD plots for Al doped α-Fe_2O_3 thin films with (a) 2% (b) 6% (c) 10% dopant concentration (*α-Fe_2O_3)

Crystallite size (*t*), strain (Cullity 1956) and dislocation density (*δ*) were calculated using Eqs. 1-3 (Kumar et al. 2011).

$$t = \frac{0.9\lambda}{B\cos\theta} \quad (1)$$

$$\delta = \frac{1}{t^2} \quad (2)$$

$$Strain = \frac{\Delta d}{d} = \frac{d_{\exp} - d_{hkl}}{d_{hkl}} \quad (3)$$

Where, *θ* is the diffraction angle, λ is the wavelength (1.5406Å) and *B* is Full Width at Half Maximum.

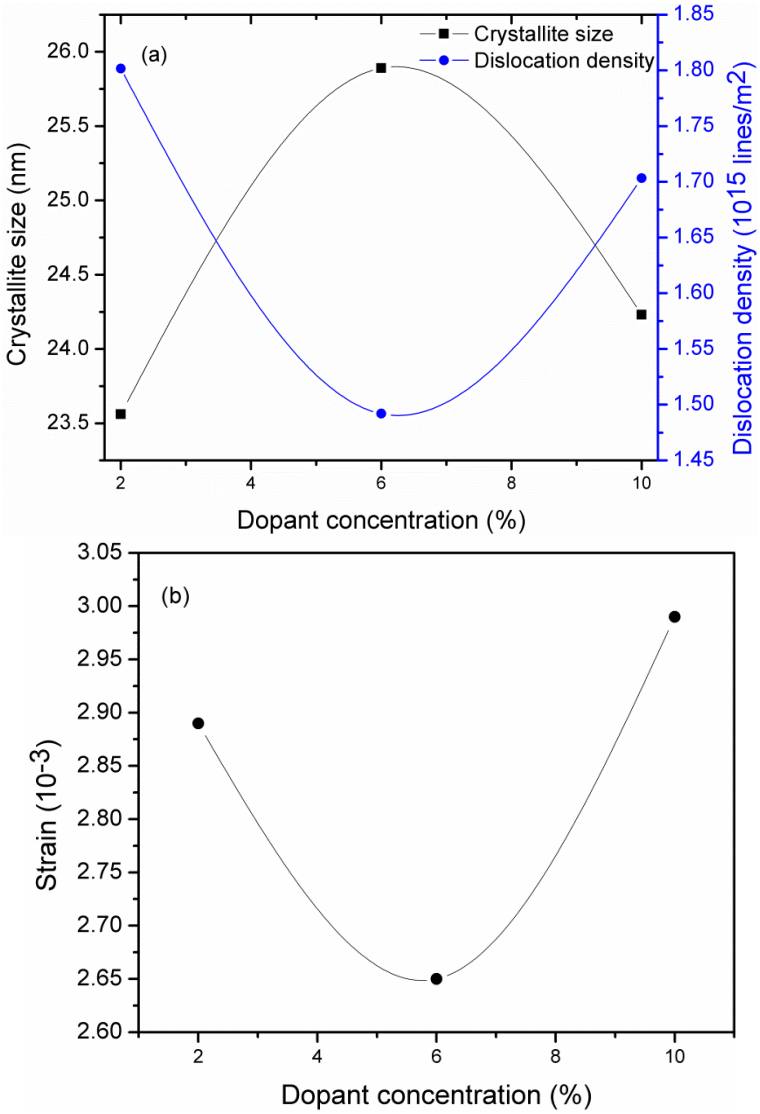

Fig. 2 (a) Crystallite size “t”, dislocation density “δ” (b) Strain as a function of dopant concentration

It can be seen in Fig. 2(a) that crystallite size increases from 23.56nm to 25.89nm with increase in dopant concentration from 2% to 6%. As dopant concentration was further increased, beyond to 6%, crystallite size dropped to 24.23nm. Increase in crystallite size till dopant concentration 6% is linked with the formation of temperature gradient. This phenomenon arises when Fe^{3+} cations are substituted with Al^{3+} cations (Riaz et al. 2015, Azam et al. 2015). This results in reduction in dislocations in thin films (Fig. 2(a)) therefore increasing the crystallite size. However, at high dopant concentration decrease in crystallite size and increase in strain is attributed to decrease in crystalline order (Biju and Wen 2013) as was observed in Fig. 1. In addition, grain size in thin films is also governed by two factors i.e. neighboring grains that have different energies due to curvature of energetic grain boundaries and strain (Riaz and Naseem 2007).

Lattice parameters "*a*, *c*" and x-ray density "*ρ,* g/cm^3" were determined using Eqs. 4-5 (Cullity 1956).

$$\sin^2\theta = \frac{\lambda^2}{3a^2}\left(h^2 + k^2 + hk\right) + \frac{\lambda^2 l^2}{4c^2} \tag{4}$$

$$\rho = \frac{1.66042\Sigma A}{V} \tag{5}$$

It can be seen in Table 1 that unit cell volume reduced as dopant concentration was increased to 10%. This shrinkage in unit cell volume is credited to difference in radii of Al^{3+} and Fe^{3+} cations. Additionally, it can be observed in Table 1 that "a" increases as dopant concentration was increased to 10% but slight decrease in "c" was observed. This effect is due to charge repulsion (Riaz et al. 2014c).

Table 1 Structural parameters for Al doped α-Fe_2O_3 thin films

Dopant concentration (%)	Lattice parameters (Å)		Unit cell volume (Å^3)	X-ray density (g/cm^3)
	a	c		
2	5.015	13.666	297.6468	5.413302
6	5.009	13.653	296.6525	5.431445
10	5.011	13.651	296.846	5.427906

Dielectric constant "ε" and tangent loss "tanδ" (Fig. 3) reduce with increase in frequency. At high frequencies they both become constant. This behavior in dielectric constant and tangent loss is ascribed to space charge effect (Hashim et al. 2012, Riaz et al. 2015). Behavior of dielectric constant and tangent loss is in agreement with Maxwell Wagner model. According to this, dielectric materials consist of grains and grain boundaries. Grain boundaries are energetic at low frequencies while grains are energetic at high frequencies. Electrons that pass the less resistive grains are collected at the grain boundaries. Consequently, high dielectric constant and tangent loss are observed at low frequencies. Dielectric constant and tangent loss are plotted as a function of dopant concentration in Fig. 3(c). It can be seen that dielectric constant increases from 49.9 to 51.73 (log *f* = 4.0) as dopant concentration was increased from 2% to 6%. Further increase in dopant concentration led to a decrease in dielectric constant to 46.8. Amongst several issues that control the dielectric constant in thin films crystallite size and strain are most significant. It has already been observed in Fig. 2(a) that crystallite size increases from 23.56nm to 25.89nm with increase in dopant concentration up to 6% that results in decrease in internal stresses (Fig. 2(b)). This increases the chances of development of 180° domains thereby leading to increase dielectric constant value and decrease in tangent loss. At high dopant concentration the enhanced stresses (Fig. 2(b)) add to the partial clamping of domain wall motion thus leading to decrease in dielectric constant (Azam et al. 2015).

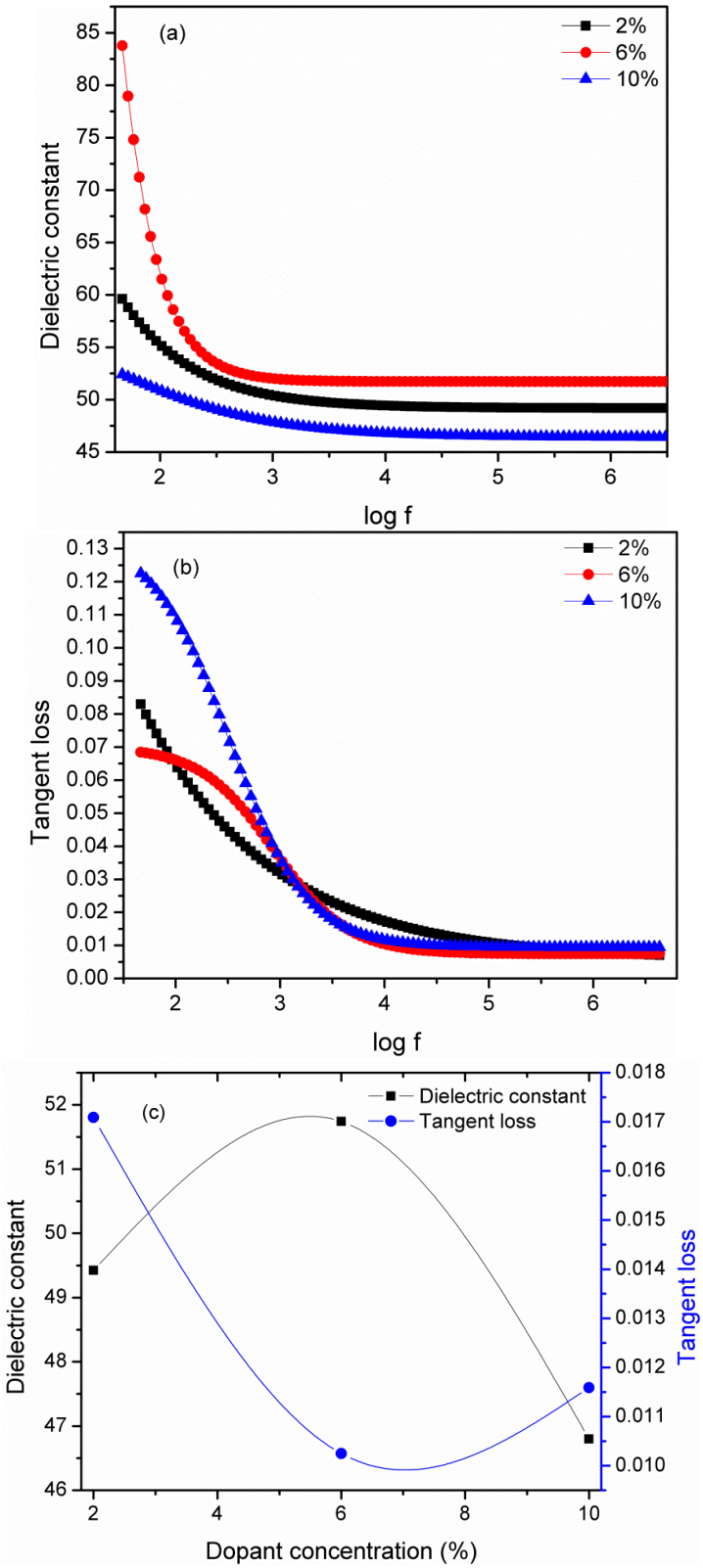

Fig. 3 Dielectric constant "ε" and tangent loss "tanδ" for Al doped iron oxide thin films as a function of log *f* (c) Dielectric constant and tangent loss plotted as a function of dopant concentration at log *f* = 4.0

An important parameter during dielectric study of thin films is the conductivity. Conductivity (σ) of Al doped iron oxide thin films was determined using Eq. 8 (Barsoukov and Macdonald 2005).

$$\sigma = 2\pi f \varepsilon \varepsilon_o \tan\delta \tag{8}$$

A.c. conductivity is plotted as a function of log *f* in Fig. 4. Conductivity remains frequency independent in low frequency region (log *f* < 4.5) and is attributed to d.c. conductivity. At high frequencies (log *f* > 4.5) conductivity increases as frequency of applied field increases and is known as a.c. conductivity of the specimen. A.c. conductivity arises due to electron hopping from one potential well to another (Hashim et al. 2012). This increase in conductivity at high frequencies can be illustrated by Koop's theory. Based on this theory increase in conductivity in high log *f* region is attributed to the presence of conducting grains (Hashim et al. 2012, Barsoukov and Macdonald 2005). It can be seen that conductivity in Al doped α-Fe_2O_3 thin films increases as Al concentration was increased thus making these films suitable as high density recording media (Shinde et al. 2011).

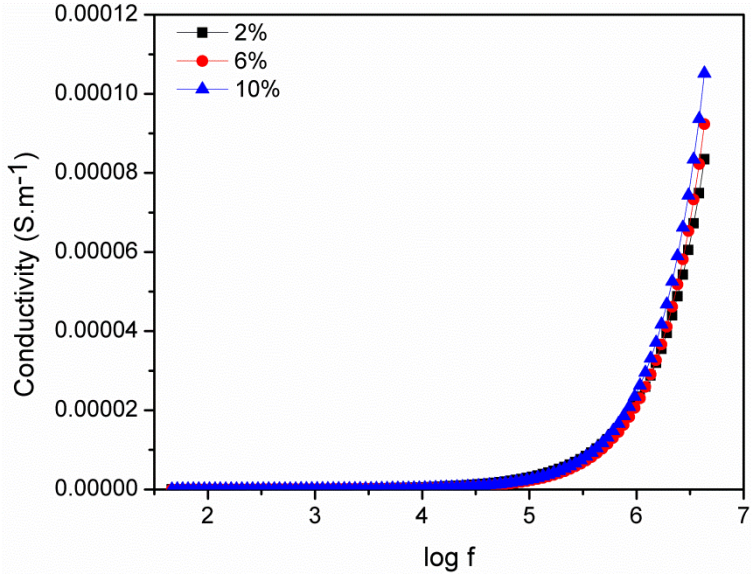

Fig. 4 Conductivity for Al doped α-Fe_2O_3 thin films

Al doped hematite (Fig. 5) thin films demonstrate ferromagnetic nature. In α-Fe_2O_3, spins in corresponding planes are laid down in parallel manner. Spins in adjoining planes are allied antiparallel to each other. Antiferromagnetic pairing occurs with adjoining planes. "*Spin-orbit pairing*" in the two adjoining planes add up to the presence of uncompensated spins of Fe^{3+} cations (Akbar et al. 2014a, Rivera et al. 2012). These uncompensated spins (Riaz et al. 2011) consequently lead to canting of spins among the planes. This results in ferromagnetic behavior in Al^{3+} doped α-Fe_2O_3 thin films. As aluminum concentration increases in Fe_2O_3 lattice, canting of spins is

greater due to divergence created by existence of aluminum. Thus, saturation magnetization increases. When dopant concentration was increased further i.e. 6%, large number of defects comprising of increased dislocations (Fig. 2) lead to insufficient arrangement of spins. This results in decrease in magnetization values (Riaz et al. 2014a, Akbar et al. 2014a).

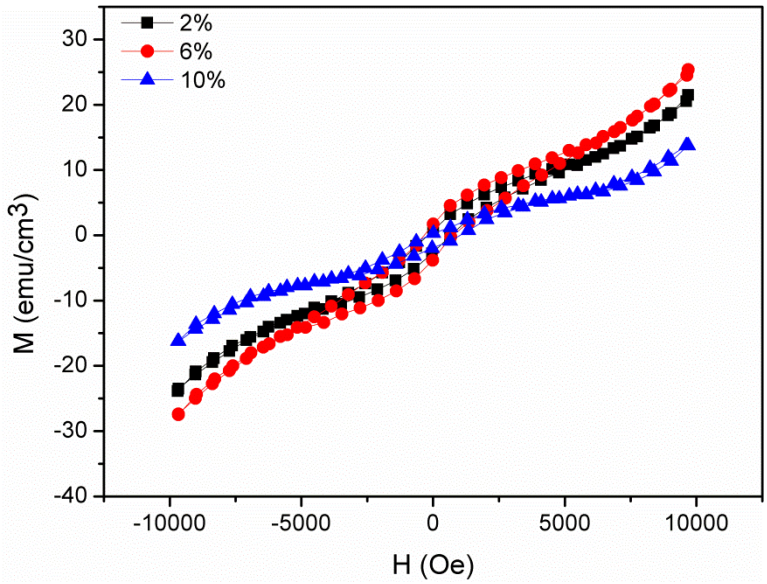

Fig. 5 Magnetic hysteresis for Al doped iron oxide thin films

4. CONCLUSIONS

Al doped α-Fe_2O_3 thin films were prepared by sol-gel and spin coating technique. Dopant concentration was varied as 2%, 6% and 10%. XRD results confirmed the structure of α-Fe_2O_3 phase. Increase in crystallite size accompanied by the decrease in stress values was observed with increase in dopant concentration up to 6%. This resulted in increase in dielectric constant from 49.9 to 51.73 (log *f* = 4.0). Conductivity in Al doped thin films increased with increase in dopant concentration thus making these films suitable for high density recording media. M-H curves showed ferromagnetic behavior with increased saturation magnetization values up to a dopant concentration of 6%.

REFERENCES

Ahn, C.W., Choi, J.J. Ryu, J. Hahn, B.D. Kim, J.W. Yoon, W.H. Choi, J.H. and Park, D.S. (2015), "Microstructure and electrochemical properties of iron oxide film fabricated by aerosol deposition method for lithium ion battery", *Journal of Pow. Sour.*, **275**, 336-340.

Akbar, A. Riaz, S. Bashir, M. and Naseem, S. (2014a), "Effect of Fe^{3+}/Fe^{2+} ratio on superparamagnetic behavior of spin coated iron oxide thin films", *IEEE Trans. Magn.*, **50**, 2200804.

Akbar, A. Riaz, S. Ashraf, R. and Naseem, S. (2014(b)), "Magnetic and magnetization properties of Co-doped Fe_2O_3 thin films", *IEEE Trans. Magn.*, **50**, 2201204

Asghar, M.H. Placido, F. and Naseem, S. (2006(a)), “Characterization of reactively evaporated TiO_2 thin films as high and medium index layers for optical applications”, *Eur. Phys. J. - Appl. Phys.*, **35**, 177-184.

Asghar, M.H. Placido, F. and Naseem, S. (2006(b)), “Characterization of Ta_2O_5 thin films prepared by reactive evaporation”, *Eur. Phys. J. - Appl. Phys.*, **36**, 119-124.

Azam. M. Riaz, S. Akbar, A. and Naseem, S. (2015), “Structural, magnetic and dielectric properties of spinel $MgFe_2O_4$ by sol–gel route”, *J. Sol-Gel Sci. Technol.*, **74**, 340–351.

Bamdad, M. and Ghotbi, M.Y. (2012), “A new approach to the synthesis of nanostructured Fe_3Al alloy and aluminum doped iron oxide material”, *Adv. Powd. Technol.*, **23**, 839–844.

Barsoukov, E. and Macdonald, J.R. (2005), “Impedance spectroscopy theory: Experiment and applications”, John Wiley & Sons, Inc., Publication, New Jersey, 2005.

Biju, Z. and Wen, H. (2013), “Influence of substrate temperature on the structural and properties of In-doped CdO films prepared by PLD”, *J. Semicond.*, **34**, 053003-1-6

Cullity, B.D. (1956), “Elements of x-ray diffraction”, Addison Wesley Publishing Company, USA.

Hashim, M. Alimuddin, Kumar, S. Koo, B.H. Shirsath, S.E. Mohammed, E.M. Shah, J. Kotnala, R.K. Choi, H.K. Chung, H. and Kumar, R. (2012), “Structural, electrical and magnetic properties of Co–Cu ferrite nanoparticles”, *J. Alloy Compd.*, **518**, 11– 18.

Huda, M.N. Walsh, A. Yan, Y. Wei, S.H. and Al-Jassim, M.M. (2010), “Electronic, structural, and magnetic effects of 3d transition metals in hematite”, *J. Appl. Phys.*, **107**, 123712.

Kment, S. Hubicka, Z. Krysa, J. Sekora, D. Zlamal, M. Olejnicek, J. Cada, M. Ksirova, P. Remes, Z. Schmuki, P. Schubert, E. and Zboril, R. (2015), “On the improvement of PEC activity of hematite thin films deposited by high-power pulsed magnetron sputtering method”, *Appl. Cataly. B: Environ.*, **165**, 344–350.

Kumar, N. Sharma, V. Parihar, U. Sachdeva, R. Padha, N. and Panchal, C.J. (2011) “Structure, optical and electrical characterization of tin selenide thin films deposited at room temperature using thermal evaporation method”, *J. Nano- Electron. Phys.*, **3**, 117-126.

Levinson, L.M. (1971), “Temperature dependence of the weak ferromagnetic moment of hematite”, *Phys. Rev. B*, **3**, 1971.

Martis, V. Oldman, R. Anderson, R. Fowles, M. Hyde, T. Smith, R. Nikitenko, S. Bras, W. and Sankar, G. (2013), “Structure and speciation of chromium ions in chromium doped Fe_2O_3 catalysts”, *Phys. Chem. Phys.*, **15**, 168-175.

Phuan, Y.W. Chong, M.N. Zhu, T. Yong, S.T. and Chan, E.S. (2015), “Effects of annealing temperature on the physicochemical, optical and photoelectrochemical properties of nanostructured hematite thin films prepared via electrodeposition method”, *Mater. Res. Bullet.*, **69**, 71–77.

Riaz, S. and Naseem, S. (2007), “Effect of reaction temperature and time on the structural properties of $Cu(In,Ga)Se_2$ thin films deposited by sequential elemental layer technique”, *J. Mater. Sci. Technol.*, **23**, 499-503.

Riaz, S. Akbar, A. and Naseem, S. (2013), “Structural, electrical and magnetic properties of iron oxide thin films”, *Adv. Sci. Lett.*, **19**, 828-833.

Riaz, S. Akbar, A. and Naseem, S. (2014a), “Ferromagnetic Effects in Cr-Doped Fe_2O_3 Thin Films”, *IEEE Trans. Magn.*, **50**, 2200704.

Riaz, S. Ashraf, R. Akbar, A. and Naseem, S. (2014b), “Free growth of iron oxide nanostructures by sol-gel spin coating technique—structural and magnetic properties”, *IEEE Trans. Magn.*, **50**, 2301805.

Riaz, S. Shah, S.M.H. Akbar, A. Kayani, Z.N. and Naseem, S. (2014c), “Effect of Bi/Fe ratio on the structural and magnetic properties of $BiFeO_3$ thin films by Sol-Gel”, *IEEE Trans. Magn.*, **50**, 2201304.

Riaz, S. Shah, S.M.H. Akbar, A. Atiq, S. and Naseem, S. (2015), “Effect of Mn doping on structural, dielectric and magnetic properties of $BiFeO_3$ thin films”, *J. Sol-Gel Sci. Technol.*, **74**, 329-339.

Riaz, S. Naseem, S. and Xu, Y.B. (2011), “Room temperature ferromagnetism in sol–gel deposited unpauli-doped ZnO films”, *J. Sol-Gel Sci. Technol.*, **59**, 584–590.

Rivera, R. Pinto, H.P. Stashans, A. and Piedra, L. (2012), “Density functional theory study of Al-doped hematite”, *Phys. Scr.*, 85, 015602.

Shimomura, N. Pati, S.P. Sato, Y. Nozaki, T. Shibata, T. Mibu, K. and Sahashi, M. (2015), “Morin transition temperature in (0001)-oriented α-Fe_2O_3 thin film and effect of Ir doping”, J. Appl. Phys., **117**, 17C736.

Shinde, S.S. Bhosale, C.H. and Rajpure, K.Y. (2011), “Studies on morphological and electrical properties of Al incorporated combusted iron oxide”, *J. Alloy Compd.*, **509**, 3943–3951.

Suresh, R. Prabu, R. Vijayaraj, A. Giribabu, K. Stephen, A. and Narayanan, V. (2012), “Facile synthesis of cobalt doped hematite nanospheres: Magnetic and their electrochemical sensing properties”, *Mater. Chem. Phys.*, **134**, 590-596.

Ubale, A.U. and Belkhedkar. M.R. (2015), “Size dependent physical properties of nanostructured α-Fe_2O_3 thin films grown by successive ionic layer adsorption and reaction method for antibacterial application,” *J. Mater. Sci. Technol.*, **31(1)**, 1-9.